

Random Subsets of Structured Deterministic Frames have MANOVA Spectra

Marina Haikin ^{*} Ram Zamir ^{*} Matan Gavish [†]

Abstract

We draw a random subset of k rows from a frame with n rows (vectors) and m columns (dimensions), where k and m are proportional to n . For a variety of important deterministic equiangular tight frames (ETFs) and tight non-ETF frames, we consider the distribution of singular values of the k -subset matrix. We observe that for large n they can be precisely described by a known probability distribution – Wachter’s MANOVA spectral distribution, a phenomenon that was previously known only for two types of random frames. In terms of convergence to this limit, the k -subset matrix from all these frames is shown to be empirically indistinguishable from the classical MANOVA (Jacobi) random matrix ensemble. Thus empirically the MANOVA ensemble offers a universal description of the spectra of randomly selected k -subframes, even those taken from deterministic frames. The same universality phenomena is shown to hold for notable random frames as well. This description enables exact calculations of properties of solutions for systems of linear equations based on a random choice of k frame vectors out of n possible vectors, and has a variety of implications for erasure coding, compressed sensing, and sparse recovery. When the aspect ratio m/n is small, the MANOVA spectrum tends to the well known Marčenko-Pastur distribution of the singular values of a Gaussian matrix, in agreement with previous work on highly redundant frames. Our results are empirical, but they are exhaustive, precise and fully reproducible.

Keywords. Deterministic frames — equiangular tight frames — MANOVA — Jacobi ensemble — restricted isometry property — Gaussian channel with erasures — Grassmannian frame — Paley frame — random Fourier — Shannon transform — analog source coding.

Consider a frame $\{\mathbf{x}_i\}_{i=1}^n \subset \mathbb{R}^m$ or \mathbb{C}^m and stack the vectors as rows to obtain the n -by- m frame matrix X . Assume that $\|\mathbf{x}_i\|_2 = 1$ (deterministic frames) or $\lim_{n \rightarrow \infty} \|\mathbf{x}_i\| = 1$ almost surely (random frames). This paper studies properties of a random subframe $\{\mathbf{x}_i\}_{i \in K}$, where K is chosen uniformly at random from

^{*}EE - Systems Department, Tel Aviv University, Tel Aviv, Israel

[†]School of Computer Science and Engineering, Hebrew University of Jerusalem

$[n] = \{1, \dots, n\}$ and $|K| = k \leq n$. We let X_K denote the k -by- m submatrix of X created by picking only the rows $\{\mathbf{x}_i\}_{i \in K}$; call this object a *typical k -submatrix* of X . We consider a collection of well-known deterministic frames, listed in Table 1, which we denote by \mathcal{X} . Most of the frames in \mathcal{X} are equiangular tight frames (ETFs), and some are near-ETFs.

This paper suggests that for a frame in \mathcal{X} it is possible to calculate quantities of the form $\mathbb{E}_K \Psi(\lambda(G_K))$, where $\lambda(G_K) = (\lambda_1(G_K), \dots, \lambda_k(G_K))$ is the vector of eigenvalues of the k -by- k Gram matrix $G_K = X_K X_K'$ and Ψ is a functional of these eigenvalues. As discussed below, such quantities are of considerable interest in various applications where frames are used, across a variety of domains, including compressed sensing, sparse recovery and erasure coding.

We present a simple and explicit formula for calculating $\mathbb{E}_K \Psi(\lambda(G_K))$ for a given frame in \mathcal{X} and a given spectral functional Ψ . Specifically, for the case $k \leq m$,

$$\mathbb{E}_K \Psi(\lambda(G_K)) \approx \Psi(f_{\beta, \gamma}^{MANOVA}),$$

where $\beta = k/m$, $\gamma = m/n$ and where $f_{\beta, \gamma}^{MANOVA}$ is the density of Wachter's classical MANOVA(β, γ) limiting distribution [27]. The fluctuations about this approximate value are given *exactly* by

$$\mathbb{E}_K |\Psi(\lambda(G_K)) - \Psi(f_{\beta, \gamma}^{MANOVA})|^2 = C n^{-b} \log^{-a}(n). \quad (1)$$

While the constant C may depend on the frame, the exponents a and b are *universal* and depend only on Ψ and on the aspect ratios β and γ . Evidently, the precision of the MANOVA-based approximation is good, known, and improves as m and k both grow proportionally to n .

Formula 1 is based on a far-reaching *universality hypothesis*: For all frames in \mathcal{X} , as well as for well-known random frames also listed in Table 1, we find that the spectrum of the typical k -submatrix ensemble is indistinguishable from that of the classical MANOVA (Jacobi) random matrix ensemble [1] of the same size. (Interestingly, it will be shown that for deterministic ETFs this indistinguishability holds in a stronger sense than for deterministic non-ETF frames.) This universality is not asymptotic, and concerns finite n -by- m frames. However, it does imply that the spectrum of the typical k -submatrix ensemble converges to a universal limiting distribution, which is non other than Wachter's MANOVA(β, γ) limiting distribution [27]. It also implies that the universal exponents a and b in (1) are previously unknown, universal quantities corresponding to the classical MANOVA (Jacobi) random matrix ensemble.

This brief announcement tests Formula 1 and the underlying universality hypothesis by conducting substantial computer experiments, in which a large number of random k -submatrices are generated. We study a large variety of deterministic frames, both real and complex. In addition to the universal object (the MANOVA ensemble) itself, we study difference-set spectrum frames, Grassmannian frames, real Paley frames, complex Paley frames, quadratic phase chirp frames, Spikes and Sines frames, and Spikes and Hadamard frames.

We report compelling empirical evidence, systematically documented and analyzed, which fully supports the universality hypothesis and (1). Our results are

empirical, but they are exhaustive, precise, reproducible and meet the best standards of empirical science.

For this purpose, we develop a natural framework for empirically testing such hypotheses regarding limiting distribution and convergence rates of random matrix ensembles. Before turning to deterministic frames, we validate our framework on well-known random frames, including real orthogonal Haar frames, complex unitary Haar frames, real random Cosine frames and complex random Fourier frames. Interestingly, rigorous proofs that identify the MANOVA distribution as the limiting spectral distribution of typical k -submatrices can be found in the literature for two of these random frames, namely the random Fourier frame [6] and the unitary Haar frame [23].

Motivation

Frames can be viewed as an analog counterpart for digital coding. They provide overcomplete representation of signals, adding redundancy and increasing immunity to noise. Indeed, they are used in many branches of science and engineering for stable signal representation, as well as error and erasure correction.

Let $\lambda(G)$ denote the vector of nonzero eigenvalues of $G = X'X$ and let $\lambda_{max}(G)$ and $\lambda_{min}(G)$ denote its max and min, respectively. Frames were traditionally designed to achieve frame bounds $\lambda_{min}(G)$ as high as possible (resp. $\lambda_{max}(G)$ as low as possible). Alternatively, they were designed to minimize *mutual coherence* [15,31], the maximal pairwise correlation between any two frame vectors.

In the passing decade it has become apparent that neither frame bounds (a global criterion) nor coherence (a local, pairwise criterion) are sufficient to explain various phenomena related to overcomplete representations, and that one should also look at collective behavior of k frame vectors from the frame, $2 \leq k \leq n$. While different applications focus on different properties of the submatrix G_K , most of these properties can be expressed as a function of $\lambda(G_K)$, and even just an average of a scalar function of the eigenvalues. Here are a few notable examples.

Restricted Isometry Property (RIP). Recovery of any $k/2$ -sparse signal $\mathbf{v} \in \mathbb{R}^n$ from its linear measurement $F'\mathbf{v}$ using ℓ_1 minimization is guaranteed if the spectral radius of $G_K - I$, namely,

$$\Psi_{RIP}(\lambda(G_K)) = \max\{\lambda_{max}(G_K) - 1, 1 - \lambda_{min}(G_K)\}, \quad (2)$$

is uniformly bounded by some $\delta < 0.4531$ on all $K \subset [n]$ [2,20,26].

Statistical RIP. Numerous authors have studied a relaxation of the RIP condition suggested in [10]. Define

$$\Psi_{StRIP,\delta}(\lambda(G_K)) = \begin{cases} 1 & \Psi_{RIP}(\lambda(G_K)) \leq \delta \\ 0 & \text{otherwise} \end{cases}. \quad (3)$$

Then $\mathbb{E}_K \Psi_{StRIP, \delta}(\lambda(G_K))$ is the probability that the RIP condition with bound δ holds when X acts on a signal supported on a random set of k coordinates.

Analog coding of a source with erasures. In [3] two of us considered a typical erasure pattern of $n - k$ random samples known at the transmitter, but not the receiver. The rate-distortion function of the coding scheme suggested in [3] is determined by $\mathbb{E}_K \log(\beta \Psi_{AC}(\lambda(G_K)))$, with

$$\Psi_{AC}(\lambda(G_K)) = \frac{1}{k} \text{tr}[(G_K)^{-1}] / \left(\frac{1}{k} \text{tr}[G_K] \right)^{-1}, \quad (4)$$

i.e., $\Psi_{AC}(\lambda(G_K))$ is the arithmetic-to-harmonic means ratio of the eigenvalues (the arithmetic mean is 1 due to the normalization of frames). This quantity is the signal amplification responsible for the excess rate of the suggested coding scheme. Note that β here is the inverse of β defined in [3].

Shannon transform. The quantity

$$\begin{aligned} \Psi_{Shannon}(\lambda(G_K)) &= \frac{1}{k} \log(\det(I + \alpha G_K)) \\ &= \frac{1}{k} \text{tr}(\log(I + \alpha G_K)), \end{aligned} \quad (5)$$

which was suggested in [4], measures the capacity of a linear-Gaussian erasure channel. Specifically, it assumes $y = XX'x + z$, (where x and y are the channel input and output) followed by $n - k$ random erasures. The quantity α in (5) is the signal-to-noise ratio $SNR = \alpha \geq 0$.

In this paper, we focus on *typical-case* performance criteria (those that seek to optimize $\mathbb{E}_K \Psi(\lambda(G_K))$ over random choice of K) rather than *worse-case* performance criteria (those that seek to optimize $\max_{K \subset [n]} \Psi(\lambda(G_K))$, such as RIP). For the remainder of this paper, $K \subset [n]$ will denote a uniformly distributed random subset of size k . Importantly, k should be allowed to be large, even as large as m .

For a given Ψ , one would like to design frames that optimize $\mathbb{E}_K \Psi(\lambda(G_K))$. This turns out to be a difficult task; in fact, it is not even known how to calculate $\mathbb{E}_K \Psi(\lambda(G_K))$ for a given frame X . Indeed, to calculate this quantity one effectively has to average Ψ over the spectrum $\lambda(G_K)$ for all $\binom{n}{k}$ subsets $K \subset [n]$. It is of little surprise to the information theorist that the first frame designs, for which performance was formally bounded (and still not calculated exactly), consisted of random vectors [14, 19–22, 24].

Random Frames

When the frame is random, namely when X is drawn from some ensemble of random matrices, the typical k -submatrix X_K is also a random matrix. Given a

specific Ψ , rather than seeking to bound $\mathbb{E}_K \Psi(\lambda(G_K))$ for specific n and m , it can be extremely rewarding to study the limit of $\Psi(\lambda(G_K))$ as the frame size n and m grow. This is because tools from random matrix theory become available, which allow exact asymptotic calculation of $\lambda(G_K)$ and $\Psi(\lambda(G_K))$, and also because their limiting values are usually very close to their corresponding values for finite n and m , even for low values of n .

Let us consider then a sequence of dimensions m_n with $m_n/n = \gamma_n \rightarrow \gamma$ and a sequence of random frame matrices $X^{(n)} \subset \mathbb{R}^{n \times m_n}$ or $\mathbb{C}^{n \times m_n}$. To characterize the collective behavior of k -submatrices we choose a sequence k_n with $k_n/m_n = \beta_n \rightarrow \beta$ and look at the spectrum $\lambda(G_{K_n})$ of the random matrix X_{K_n} as $n \rightarrow \infty$, where $K_n \subset [n]$ is a randomly chosen subset with $|K_n| = k_n$. Here and below, to avoid cumbersome notation we omit the subscript n and write m, k and K for m_n, k_n and K_n .

A mainstay of random matrix theory is the celebrated convergence of the empirical spectral distribution of random matrices, drawn from a certain ensemble, to a limiting spectral distribution corresponding to that ensemble. This has indeed been established for three random frames:

1. *Gaussian i.i.d frame*: Let $X_{normal}^{(n)}$ have i.i.d normal entries with mean zero and variance $1/m$. The empirical distribution of $\lambda(G_K)$ famously converges, almost surely in distribution, to the Marčenko-Pastur density [13] with parameter β :

$$f_{\beta}^{MP}(x) = \frac{\sqrt{(x - \lambda_-^{MP})(\lambda_+^{MP} - x)}}{2\beta\pi x} \cdot I_{(\lambda_-^{MP}, \lambda_+^{MP})}(x), \quad (6)$$

supported on $[\lambda_-^{MP}, \lambda_+^{MP}]$ where $\lambda_{\pm}^{MP} = (1 \pm \sqrt{\beta})^2$. Moreover, almost surely $\lambda_{max}(G_{normal}^{(n)}) \rightarrow \lambda_+$ and $\lambda_{min}(G_{normal}^{(n)}) \rightarrow \lambda_-$; in other words, the maximal and minimal empirical eigenvalues converge almost surely to the edges of the support of the limiting spectral distribution [28].

2. *Random Fourier frame*: Consider the random Fourier frame, in which the m_n columns of $X_{fourier}^{(n)}$ are drawn uniformly at random from the columns of the n -by- n discrete Fourier transform (DFT) matrix (normalized s.t absolute value of matrix entries is $1/\sqrt{m}$). Farrell [6] has proved that the empirical distribution of $\lambda(G_K)$ converges, almost surely in distribution, as $n \rightarrow \infty$ and as m and k grow proportionally to n , to the so-called MANOVA limiting distribution, which we now describe briefly.

The classical MANOVA(n, m, k, \mathcal{F}) ensemble¹, with $\mathcal{F} \in \{\mathbb{R}, \mathbb{C}\}$ is the distribution of the random matrix

$$\frac{n}{m}(AA' + BB')^{-\frac{1}{2}}BB'(AA' + BB')^{-\frac{1}{2}}, \quad (7)$$

where $A_{k \times (n-m)}, B_{k \times m}$ are random standard Gaussian i.i.d matrices with entries in \mathcal{F} . Wachter [27] discovered that, as $k/m \rightarrow \beta \leq 1$ and $m/n \rightarrow \gamma$, the

¹Also known as the beta-Jacobi ensemble with beta=1 (orthogonal) for $\mathcal{F} = \mathbb{R}$, and beta=2 (unitary) for $\mathcal{F} = \mathbb{C}$.

empirical spectral distribution of the MANOVA(n, m, k, \mathbb{R}) ensemble converges, almost surely in distribution, to the so-called MANOVA(β, γ) limiting spectral distribution², whose density is given by

$$f_{\beta, \gamma}^{MANOVA}(x) = \frac{\sqrt{(x - r_-)(r_+ - x)}}{2\beta\pi x(1 - \gamma x)} \cdot I_{(r_-, r_+)}(x) + \left(1 + \frac{1}{\beta} - \frac{1}{\beta\gamma}\right)^+ \cdot \delta\left(x - \frac{1}{\gamma}\right) \quad (8)$$

where $(x)^+ = \max(0, x)$. The limiting MANOVA distribution is compactly supported on $[r_-, r_+]$ with

$$r_{\pm} = \left(\sqrt{\beta(1 - \gamma)} \pm \sqrt{1 - \beta\gamma}\right)^2. \quad (9)$$

The same holds for the MANOVA(n, m, k, \mathbb{C}) ensemble.

Note that the support of the MANOVA(β, γ) distribution is smaller than that of the corresponding Marčenko-Pastur law for the same aspect ratios. Figure 1 shows these two densities for $\beta = 0.8$ and $\gamma = 0.5$. Nevertheless, as the MANOVA dimension ratio becomes small, its distribution tends to the Marčenko-Pastur distribution (6), i.e., $f_{\beta, \gamma}^{MANOVA}(x) \rightarrow f_{\beta}^{MP}(x)$ as $\gamma \rightarrow 0$. Thus, a highly redundant random Fourier frame behaves like a Gaussian i.i.d. frame.

3. *Unitary Haar frame:* Let $X_{\text{haar}}^{(n)}$ consist of the first m columns of a Haar-distributed n -by- n unitary matrix normalized by $\sqrt{n/m}$ (the Haar distribution being the uniform distribution over the group of n -by- n unitary matrices). Edelman and Sutton [23] proved that the empirical spectral distribution of $\lambda(G_K)$ also converges, almost surely in distribution, to the MANOVA limiting spectral distribution (See also [27] and the closing remarks of [6].)

The maximal and minimal eigenvalues of a matrix from the MANOVA(n, m, k, \mathcal{F}) ensemble ($\mathcal{F} \in \{\mathbb{R}, \mathbb{C}\}$) are known to converge almost surely to r_+ and r_- , respectively [11]. While we are not aware of any parallel results for the random Fourier and Haar frames, the empirical evidence in this paper show that it must be the case.

These random matrix phenomena have practical significance for evaluations of functions of the form $\Psi(\lambda(G_K))$ such as those mentioned above. The functions Ψ_{AC} and Ψ_{Shannon} , for example, are what [29] call *linear spectral statistics*, namely functions of $\lambda(G_K)$ that may be written as an integral of a scalar function against the empirical measure of $\lambda(G_K)$. Convergence of the empirical distribution of

²The literature uses the term MANOVA to refer both to the random matrix ensemble, which we denote here by MANOVA(n, m, k, \mathcal{F}), and to the limiting spectral distribution, which we denote here by MANOVA(β, γ).

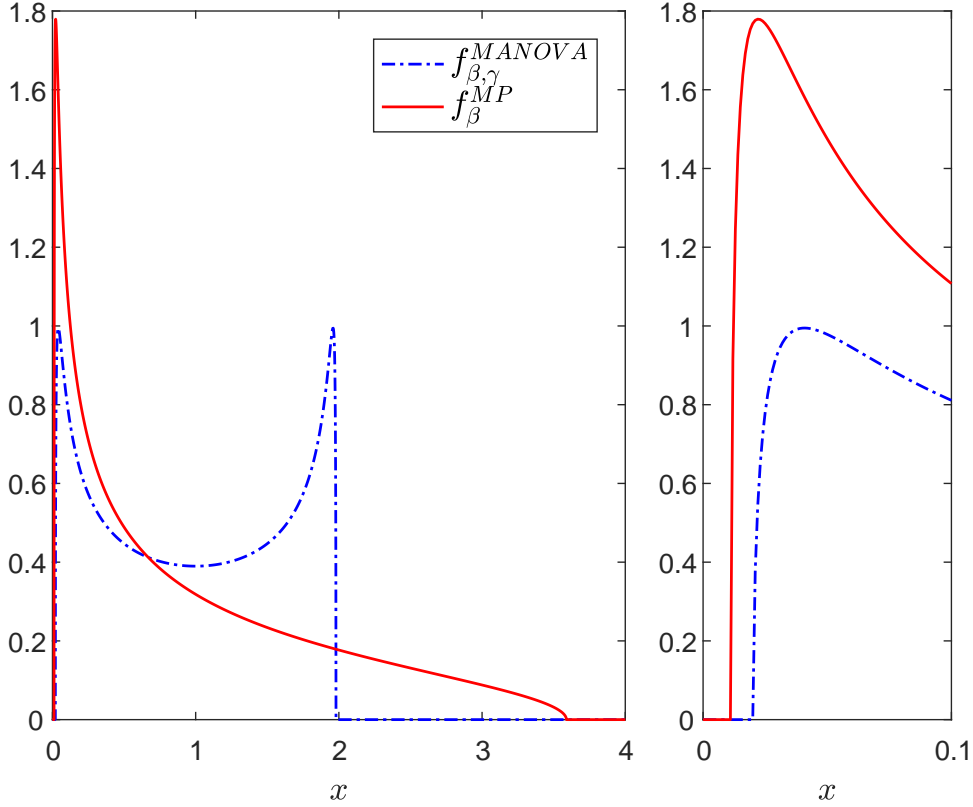


Figure 1: Limiting MANOVA ($\beta = 0.8, \gamma = 0.5$) and Marčenko-Pastur ($\beta = 0.8$) density functions. Left: density on the interval $x \in [0, 4]$. Right: Zoom in on the interval $x \in [0, 0.1]$.

$\lambda(G_K^{(n)})$ to the limiting MANOVA distribution with density $f_{\beta, \gamma}^{MANOVA}$ implies

$$\begin{aligned} \lim_{n \rightarrow \infty} \Psi_{AC}(\lambda(G_{K_n}^{(n)})) &= \int \frac{1}{x} f_{\beta, \gamma}^{MANOVA}(x) dx \\ \lim_{n \rightarrow \infty} \Psi_{Shannon}(\lambda(G_{K_n}^{(n)})) &= \int \log(1 + \alpha x) f_{\beta, \gamma}^{MANOVA}(x) dx \end{aligned} \quad (10)$$

for both the random Fourier and Haar frames; the integrals on the right hand side may be evaluated explicitly. Similarly, convergence of $\lambda_{max}(G_K)$ and $\lambda_{min}(G_K)$ to r_+ and r_- implies, for example, that

$$\lim_{n \rightarrow \infty} \Psi_{RIP}(\lambda(G_K^{(n)})) = \max(r_+ - 1, 1 - r_-). \quad (11)$$

To demonstrate why such calculations are significant, we note that Equations (10) and (11) immediately allow us to compare the Gaussian i.i.d frame with the random Fourier and Haar frames, in terms of their limiting value of functions of interest. Figure 2 compares the limiting value of Ψ_{RIP} , Ψ_{AC} and $\Psi_{Shannon}$ over varying values of $\beta = \lim_{n \rightarrow \infty} k/m$. The plots clearly demonstrate that frames whose typical k -submatrix exhibits a MANOVA spectrum, are superior to frames whose typical k -submatrix exhibits a Marčenko-Pastur spectrum, across the performance measures.

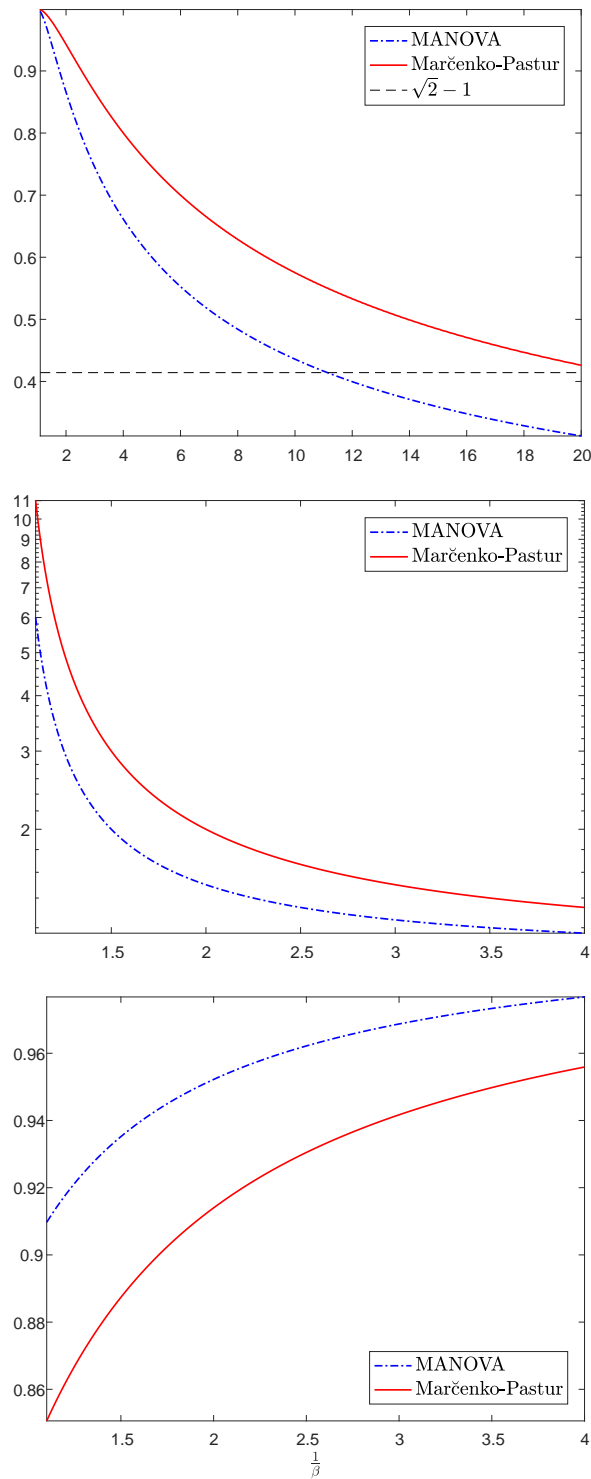


Figure 2: Comparison of limiting values of $\mathbb{E}_K \Psi(\lambda(G_K))$ for the three functions Ψ discussed in Motivation Section between the Marčenko-Pastur limiting distribution and the MANOVA distribution. Left: Ψ_{RIP} (lower is better). Middle: Ψ_{AC} (lower is better). Right: $\Psi_{Shannon}$ (higher is better).

Table 1: Frames under study

| Label | Name | \mathbb{R} or \mathbb{C} | Natural γ | Tight frame | Equiangular | References |
|-----------------------------|------------------------------|------------------------------|------------------|-------------|-------------|--------------------------|
| Deterministic frames | | | | | | |
| DSS | Difference-set spectrum | \mathbb{C} | | Yes | Yes | [7] |
| GF | Grassmannian frame | \mathbb{C} | 1/2 | Yes | Yes | [8, Cor. 2.6b] |
| RealPF | Real Paley's construction | \mathbb{R} | 1/2 | Yes | Yes | [8, Cor. 2.6a] |
| ComplexPF | Complex Paley's construction | \mathbb{C} | 1/2 | Yes | Yes | [9] |
| Alltop | Quadratic Phase Chirp | \mathbb{C} | 1/L | Yes | No | [5, eq. S4] with $L = 2$ |
| SS | Spikes and Sines | \mathbb{C} | 1/2 | Yes | No | [31] |
| SH | Spikes and Hadamard | \mathbb{R} | 1/2 | Yes | No | [31] |
| Random frames | | | | | | |
| HAAR | Unitary Haar frame | \mathbb{C} | | Yes | No | [6, 23] |
| RealHAAR | Orthogonal Haar frame | \mathbb{R} | | Yes | No | [23] |
| RandDFT | Random Fourier transform | \mathbb{C} | | Yes | No | [6] |
| RandDCT | Random Cosine transform | \mathbb{R} | | Yes | No | |

Deterministic Frames: Universality Hypothesis

Deterministic frames, namely frames whose design involves no randomness, have so far eluded this kind of asymptotically exact analysis. While there are results regarding RIP [17, 18] and statistical RIP [10, 12, 16], for example, of deterministic frame designs, they are mostly focused on highly redundant frames ($\gamma \rightarrow 0$) and the wide submatrix ($\beta \rightarrow 0$) case, where the spectrum tends to the Marčenko-Pastur distribution. Furthermore, nothing analogous, say, to the precise comparisons of Figure 2 exists in the literature to the best of our knowledge. Specifically, no results analogous to (10) and (11) are known for deterministic frames, let alone the associated convergence rates, if any.

In order to subject deterministic frames to an asymptotic analysis, we shift our focus from a single frame X to a family of deterministic frames $\{X^{(n)}\}$ created by a common construction. The frame matrix $X^{(n)}$ is n -by- m . Each frame family determines allowable sub-sequences (n, m) ; to simplify notation, we leave the subsequence implicit and index the frame sequence simply by n . The frame family also determines the aspect ratio limit $\gamma = \lim_{n \rightarrow \infty} m/n$. In what follows we also fix a sequence k with $\beta = \lim_{n \rightarrow \infty} k/m$, and let $K \subset [n]$ denote a uniformly distributed random subset.

Frames under study. The different frames that we studied are listed in Table 1, in a manner inspired by [5]. In addition to our deterministic frames of interest (the set \mathcal{X}), the table contains also two examples of random frames (real and complex variant for each), for validation and convergence analysis purposes.

Functionals under study. We studied the functionals Ψ_{StRIP} from (3), Ψ_{AC} from (4), $\Psi_{Shannon}$ from (5). In addition, we studied the maximal and minimal eigen-

values of G_K , and its condition number:

$$\begin{aligned}\Psi_{max}(\lambda(G_K)) &= \lambda_{max}(G_K) \\ \Psi_{min}(\lambda(G_K)) &= \lambda_{min}(G_K) \\ \Psi_{cond}(\lambda(G_K)) &= \lambda_{max}(G_K)/\lambda_{min}(G_K).\end{aligned}$$

Measuring the rate of convergence. In order to quantify the rate of convergence of the entire spectrum of the k -by- m matrix X_K , which is a k -submatrix of an n -by- m frame matrix X , to a limiting distribution, we let $F[X_K]$ denote the empirical cumulative distribution function (CDF) of $\lambda(G_K)$, and let $F_{\beta,\gamma}^{MANOVA}(x) = \int_{r_-}^x f_{\beta,\gamma}^{MANOVA}(x)dx$ denote the CDF of the MANOVA(β, γ) limiting distribution. The quantity

$$\Delta_{KS}(X_K) = \|F[X_K] - F_{\beta_n,\gamma_n}^{MANOVA}\|_{KS},$$

where $\|\cdot\|_{KS}$ is the Kolmogorov-Smirnov (KS) distance between CDFs, measures the distance to the hypothesised limit. Here, $\beta_n = k/m$ and $\gamma_n = m/n$ are the actual aspect ratios for the matrix X_K at hand. As a baseline we use $\Delta_{KS}(Y_{n,m,k,\mathcal{F}})$, where $Y_{n,m,k,\mathcal{F}}$ is a matrix from the MANOVA(n, m, k, \mathcal{F}) ensemble, with $\mathcal{F} = \mathbb{R}$ if X_K is real and $\mathcal{F} = \mathbb{C}$ if complex. Figure 3 illustrates the KS-distance between an empirical CDF and the limiting MANOVA CDF

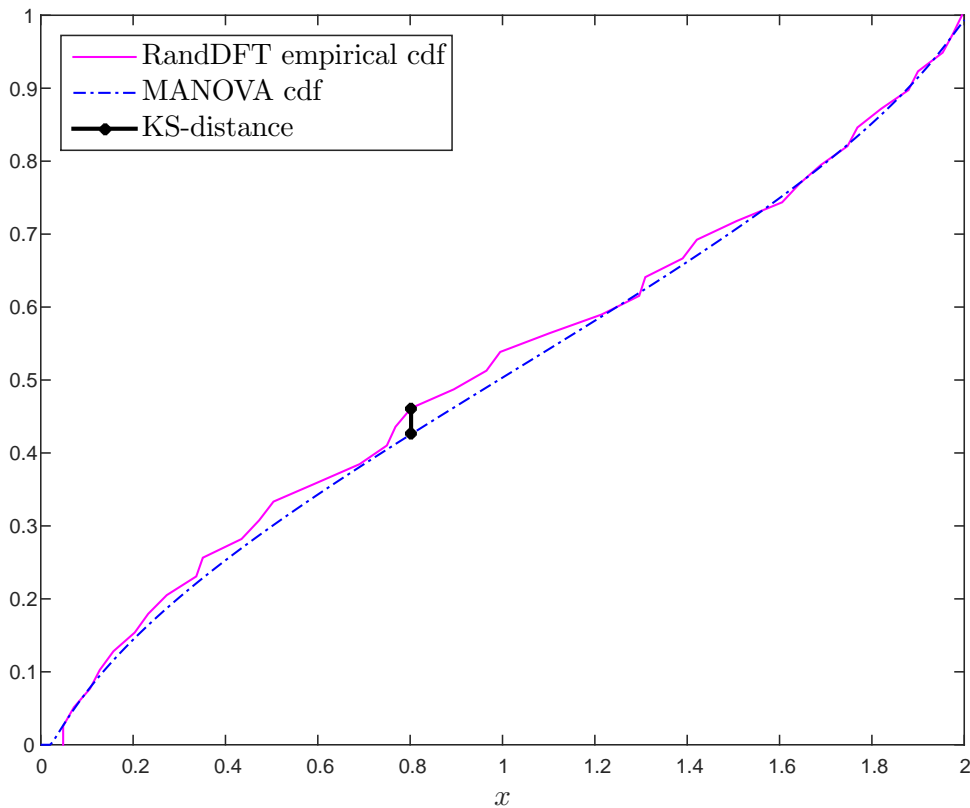


Figure 3: KS-distance of random DFT subframe, $\beta = 0.8$, $\gamma = 0.5$, $n = 100$.

Similarly, in order to quantify the rate of convergence of a functional Ψ , the quantity

$$\Delta_{\Psi}(X_K; n, m, k) = |\Psi(\lambda(G_K)) - \Psi(f_{\beta, \gamma}^{MANOVA})|$$

is the distance between the measured value of Ψ on a given k -submatrix X_K and its hypothesised limiting value. For a baseline we can use $\Delta_{\Psi}(Y_{n, m, k, \mathcal{F}})$, with $\mathcal{F} = \mathbb{R}$ if X_K is real and $\mathcal{F} = \mathbb{C}$ if complex. For linear spectral functionals like Ψ_{AC} and $\Psi_{Shannon}$, which may be written as $\Psi(\lambda(G_K)) = \int \psi dF[X_K]$ for some kernel ψ , we have $\Psi(f_{\beta, \gamma}^{MANOVA}) = \int \psi dF_{\beta, \gamma}^{MANOVA}$. For Ψ_{RIP} that depends on $\lambda_{max}(G_K)$ and $\lambda_{min}(G_K)$ we have $\Psi_{RIP}(f_{\beta, \gamma}^{MANOVA}) = \max\{r_+ - 1, 1 - r_-\}$.

Universality Hypothesis. The contributions of this paper are based on the following assertions on the typical k -submatrix ensemble X_K corresponding to a frame family $X^{(n)}$. This family may be random or deterministic, real or complex.

- H1** *Existence of a limiting spectral distribution.* The empirical spectral distribution of $X_K^{(n)}$, namely the distribution of $\lambda(G_K^{(n)})$, converges, as $n \rightarrow \infty$, to a compactly-supported limiting distribution; furthermore, $\lambda_{max}(G_K^{(n)})$ and $\lambda_{min}(G_K^{(n)})$ converge to the edges of that compact support.
- H2** *Universality of the limiting spectral distribution.* The limiting spectral distribution of $X_K^{(n)}$ is the MANOVA(β, γ) distribution [27] whose density is (8). Also $\lambda_{max}(G_K^{(n)}) \rightarrow r_+$ and $\lambda_{min}(G_K^{(n)}) \rightarrow r_-$ where r_{\pm} is given by (9).
- H3** *Exact power-law rate of convergence for the entire spectrum.* The spectrum of $X_K^{(n)}$ converges to the limiting MANOVA(β, γ) distribution

$$\left(\mathbb{E}_{K_n} \left(\Delta_{KS}(X_K^{(n)}) \right) \right)^2 \searrow 0$$

and in fact its fluctuations are given by the law

$$Var_K(\Delta_{KS}(X_K^{(n)})) = Cn^{-2b} \quad (12)$$

for some constants C, b , which may depend on the frame family.

- H4** *Universality of the rate of convergence for the entire spectrum of ETFs.* For an equiangular tight frame (ETF) family, the exponent b in (12) is universal and does not depend on the frame. Furthermore, (12) also holds, with the same universal exponent, replacing $G_K^{(n)}$ with a same-sized matrix from the MANOVA(n, m, k, \mathcal{F}) distribution defined in (7), with $\mathcal{F} = \mathbb{R}$ if $X^{(n)}$ is a real frame family, and $\mathcal{F} = \mathbb{C}$ if complex. In other words, the universal exponent b for ETFs is a property of the MANOVA (Jacobi) random matrix ensemble.
- H5** *Exact power-law rate of convergence for functionals.* For a “nice” functional Ψ , the value of $\Psi(\lambda(G_K^{(n)}))$ converges to $\Psi(f_{\beta, \gamma}^{MANOVA})$ according to the law

$$\mathbb{E}_K(\Delta_{\Psi}(X_K^{(n)})^2) = Cn^{-b} \log^{-a}(n) \quad (13)$$

for some constants C, b, a .

H6 *Universality of the rate of convergence for functionals.* While the constant C in (13) may depend on the frame, the exponents a, b are universal. (13) also holds, with the same universal exponents, replacing $G_K^{(n)}$ with a same-sized matrix from the MANOVA(n, m, k, \mathcal{F}) ensemble defined in (7), with $\mathcal{F} = \mathbb{R}$ if $X^{(n)}$ is a real frame family, and $\mathcal{F} = \mathbb{C}$ if complex. In other words, the universal exponents a, b are a property of the MANOVA (Jacobi) random matrix ensemble.

Nonstandard aspect ratio $\beta > 1$. While the classical MANOVA ensemble and limiting density are not defined for $\beta > 1$, in our case it is certainly possible to sample $k > m$ vectors from the n possible frame vectors, resulting in a situation with $\beta > 1$. In this situation, the hypotheses above require slight modifications. Specifically, the limiting spectral distribution of $X_K^{(n)}$, for $\beta > 1$, is

$$\left(1 - \frac{1}{\beta}\right) \delta(x) + f_{\beta, \gamma}^{MANOVA}(x), \quad (14)$$

where $f_{\beta, \gamma}^{MANOVA}(x)$ is the function (no longer a density) defined in (8). The rate of convergence of the distribution of nonzero eigenvalues to the limiting density $\frac{1}{\beta} f_{\frac{1}{\beta}, \beta\gamma}^{MANOVA}(\frac{1}{\beta}x) = \beta f_{\beta, \gamma}^{MANOVA}(x)$ is compared with the baseline $\beta \cdot Y_{n, k, m, \mathcal{F}}$, where $Y_{n, k, m, \mathcal{F}}$ is a matrix from the MANOVA(n, k, m, \mathcal{F}) ensemble (i.e., with reversed order of k and m).

Methods

The software we developed has been permanently deposited in the Data and Code Supplement [39]. As many of the deterministic frames under study are only defined for $\gamma = 0.5$, we primarily studied the aspect ratios ($\gamma = 0.5, \beta$) with $\beta \in \{0.3, 0.5, 0.6, 0.7, 0.8, 0.9\}$. In addition, we inspected all frames under study that are defined for the aspect ratios ($\gamma = 0.25, \beta = 0.6$) and ($\gamma = 0.25, \beta = 0.8$) (all random frames, as well as DSS and Alltop). We also studied nonstandard aspect ratios $\beta > 1$ as described in the Supporting Information [40]. For deterministic frames, n took allowed values in the range (240, 2000), ($2^5, 2^{12}$) for Grassmannian and Spikes and Hadamard frames and (600, 4000) for DSS frame with $\gamma = 0.25$. For random frames and MANOVA ensemble we used dense grid of values in the range (240, 2000). Hypothesis testing as discussed below, was based on a subset of these values where $n \geq 1000$. For each of the frame families under study, and for each value of β and γ under study, we selected a sequence (n, m, k) . The values n and m were selected so that m/n will be as close as possible to γ , however due to different aspect ratio constrains by the different frames occasionally we had m/n close but not equal to γ . We then determined k such that k/m will be as close as possible to β . For each n , we generated a single n -by- m frame matrix $X^{(n)}$. We then produced T independent samples from the uniform distribution on k_n -subsets, $K[1], \dots, K[T] \subset [n]$, and generated their corresponding k -submatrices

$X_{K[i]}^{(n)}$ ($1 \leq i \leq T$). Importantly, all these are submatrices of the same frame matrix $X^{(n)}$. We calculated $\overline{\Delta}_{KS}^{Var}(X_K^{(n)}) = \overline{\Delta}_{KS}^2(X_K^{(n)}) - \overline{\Delta}_{KS}^2(X_K^{(n)})$, the empirical variance of $\Delta_{KS}(X_{K[i]}^{(n)})$, and $\overline{\Delta}_{KS}^2(X_K^{(n)})$, the average value of $\Delta_{KS}^2(X_{K[i]}^{(n)})$ on $1 \leq i \leq T$, as a monte-carlo approximation to the left-hand side of (12), variance and MSE respectively. For each of the functionals under study, we also calculated $\overline{\Delta}_{\Psi}^2(X_{K[i]}^{(n)})$, the average value of $\Delta_{\Psi}^2(X_{K[i]}^{(n)})$ on $1 \leq i \leq T$, as a monte-carlo approximation to the left-hand side of (13).

Separately, for each triplet (n, m, k) and $\mathcal{F} \in \{\mathbb{R}, \mathbb{C}\}$ we have performed T independent draws from the MANOVA(n, m, k, \mathcal{F}) ensembles (7) and calculated analogous quantities $\overline{\Delta}_{KS}^{Var}(Y_{n,m,k,\mathcal{F}})$, $\overline{\Delta}_{KS}^2(Y_{n,m,k,\mathcal{F}})$ and $\overline{\Delta}_{\Psi}^2(Y_{n,m,k,\mathcal{F}})$.

Test 1: Testing H1–H4. For each of the frames under study and each value of (β, γ) , we computed the KS-distance for $T = 10^4$ submatrices and performed simple linear regression of $-\frac{1}{2} \log(\overline{\Delta}_{KS}^{Var}(X_K^{(n)}))$ on $\log(n)$ with an intercept. We obtained the estimated linear coefficient \hat{b} as an estimate for the exponent b , and its standard error $\sigma(\hat{b})$. Similarly we regressed $-\frac{1}{2} \log(\overline{\Delta}_{KS}^{Var}(Y_{n,m,k,\mathcal{F}}))$ on $\log(n)$ to obtain \hat{b}_{MANOVA} and $\sigma(\hat{b}_{MANOVA})$. We performed Student's t-test to test the null hypotheses $b = b_{MANOVA}$ using the test statistic

$$t = \frac{\hat{b} - b_{MANOVA}}{\sqrt{\sigma(\hat{b})^2 + \sigma(\hat{b}_{MANOVA})^2}}.$$

Under the null hypothesis, the test statistic is distributed $t_{(N+N_{MANOVA}-4)}$, where N, N_{MANOVA} are the numbers of different values of n for which we have collected the data for a frame and the MANOVA ensemble respectively. We report the R^2 of the linear fit; the slope coefficient \hat{b} and its standard error; and the p-value of the above t-test. We next regressed $-\log(\overline{\Delta}_{KS}^2)$ on $\log(n)$. Since $\overline{\Delta}_{KS}^2 = (\overline{\Delta}_{KS})^2 + \overline{\Delta}_{KS}^{Var}$, a linear fit verifies that $(\overline{\Delta}_{KS})^2 \searrow 0$.

Test 2: Testing H5–H6. For each of the frames under study, each of the functionals Ψ under study, and each value of (β, γ) , we computed the empirical value of the functionals on $T = 10^3$ submatrices. We first performed linear regression of $-\log(\overline{\Delta}_{\Psi}^2(Y_{n,m,k,\mathcal{F}}))$ on $\log(n)$ and $\log(\log(n))$ with an intercept, for $\mathcal{F} \in \{\mathbb{R}, \mathbb{C}\}$. Let a_0 denote the fitted coefficient for $\log(n)$ and let b_0 denote the fitted coefficient for $\log(\log(n))$. This step was based on triplets (n, m, k) yielding accurate aspect ratios in the range $240 \leq n \leq 2000$. We then performed simple linear regression of $-\log(\overline{\Delta}_{\Psi}^2(X_K^{(n)}; n, m, k))$ on $\log(n) + (a_0/b_0) \cdot \log(\log(n))$. The estimated linear regression coefficient \hat{b} is the estimate for the exponent b in (13), and $\sigma(\hat{b})$ is its standard error. We used $\hat{b} \cdot (a_0/b_0)$ as an estimate for the exponent a in (13). We proceeded as above to test the null hypothesis $b = b_0$. We report the R^2 of the

linear fit; the slope coefficient \hat{b} and its standard error; and the p-value of the test above.

Computing. To allow the number of monte-carlo samples to be as large as $T = 10^4$ and n to be as large as 2000, we used a large Matlab cluster running on Amazon Web Services. We used 32-logical core machines, with 240GB RAM each, which were running several hundred hours in total. The code we executed has been deposited [39]; it may easily be executed for smaller values of T and n on smaller machines.

Results

The raw results obtained in our experiments, as well as the analysis results of each experiment, have been deposited with their generating code [39].

For space considerations, the full documentation of our results is deferred to the Supporting Information [40]. To offer a few examples, Figure 4 and Table 2 show the linear fit to $\overline{\Delta}_{KS}^{Var}$ for $(\gamma = 0.5, \beta = 0.8)$. Figure 5 shows the linear fit to $\overline{\Delta}_{KS}^{Var}$ for a different value of β , namely $(\gamma = 0.5, \beta = 0.6)$. Figure 6 shows the linear fit to $\overline{\Delta}_{\Psi_{AC}}$ for $(\gamma = 0.5, \beta = 0.8)$. Figure 7 and Table 3 show the linear fit to $\overline{\Delta}_{\Psi_{Shannon}}$ for $(\gamma = 0.5, \beta = 0.8)$. Similar figures and tables for the other values (γ, β) , in particular, $(\beta = 0.3, \gamma = 0.5)$, $(\beta = 0.5, \gamma = 0.5)$, $(\beta = 0.7, \gamma = 0.5)$, $(\beta = 0.9, \gamma = 0.5)$, $(\beta = 0.6, \gamma = 0.25)$, $(\beta = 0.8, \gamma = 0.25)$, are deferred to the Supporting Information. Note that in all coefficient tables, both those shown here and those deferred to the Supporting Information, upper box shows complex frames (with t-test comparison to the complex MANOVA ensemble of the same size, denoted “MANOVA”) and bottom box shows real frames (with t-test comparison to the real MANOVA ensemble of the same size, denoted “RealMANOVA”). In each box, top rows are deterministic frames and bottom rows are random frames. Further note that in plots for Test 2 the horizontal axis is slightly different for real and complex frames, as the preliminary step described above was performed separately for real and complex frames. In the interest of space, we plot all frames over the horizontal axis calculated for complex frames.

Validation on random frames. While our primary interest was in deterministic frames, we included in the frames under study random frames. For the complex Haar frame and random Fourier frame, convergence of the empirical CDF of the spectrum to the limiting $\text{MANOVA}(\beta, \gamma)$ distribution has been proved in [6, 23]. To our surprise, not only was our framework validated on the four random frames under study, in the sense of asymptotic empirical spectral distribution, but all universality hypotheses **H1–H6** were accepted (not rejected at the 0.001 significance level, with very few exceptions).

Test results on deterministic frames. A tabular summary of our results, per hypothesis and per frame under study, is included for convenience in the Supporting Information. Universality Hypotheses **H1–H3** were accepted on all deterministic frames. For **H1–H2**, convergence of the empirical spectral distribution to the $\text{MANOVA}(\beta, \gamma)$ limit has been observed in all cases. For **H3**, the linear fit in all cases was excellent with $R^2 > 0.99$ without exception, confirming the power law in (12) and the polynomial decrease of $\overline{\Delta}_{KS}^2$ with n . Universality Hypothesis **H4** was accepted (not rejected) for deterministic equiangular tight frames (ETFs) at the 0.001 significance level, with few exceptions (see Table 2 below, as well as full results and summary table in the Supporting Information); it was rejected for deterministic non-ETFs. For $\gamma = 0.25$, Hypothesis **H4** has also been accepted for the Alltop frame, see Supporting Information. Universality Hypothesis **H5** was accepted for all deterministic frames, with excellent linear fits ($R^2 > 0.97$ without exception), confirming the power law in (13). Universality Hypothesis **H6** was accepted (not rejected) at the 0.001 significance level (and even 0.05 with few exceptions) for all deterministic frames. For the reader’s convenience, Table 4 summarizes the universal exponents for convergence of the entire spectrum (**H4**) and the universal exponents for convergence of the functionals under study (**H6**), for $(\beta, \gamma) = (0.8, 0.5)$. The framework developed in this paper readily allows tabulation of these new universal exponents for any value of (β, γ) . We have observed that the universal exponents are slightly sensitive to the random seed. However, exact evaluation of this variability requires very significant computational resources and is beyond our present scope. Similarly, some sensitivity of the p-values to random seed has been observed.

| Frame | R^2 | \hat{b} | $SE(\hat{b})$ | p-value $b = b_{\text{MANOVA}}$ |
|------------|---------|-----------|---------------|------------------------------------|
| MANOVA | 0.99828 | 0.92505 | 0.00690 | 1 |
| DSS | 0.99858 | 0.93652 | 0.00911 | 0.32089 |
| GF | 0.99921 | 0.92474 | 0.02608 | 0.99082 |
| ComplexPF | 0.99950 | 0.92454 | 0.00535 | 0.95390 |
| Alltop | 0.98906 | 0.49660 | 0.00883 | 9.4651e-47 |
| SS | 0.98767 | 0.47354 | 0.00950 | 5.8136e-45 |
| HAAR | 0.99736 | 0.94421 | 0.00873 | 0.09019 |
| RandDFT | 0.99544 | 0.94127 | 0.01644 | 0.36788 |
| RealMANOVA | 0.99873 | 0.95610 | 0.00613 | 1 |
| RealPF | 0.99871 | 0.91244 | 0.00821 | 9.7174e-05 |
| SH | 0.99989 | 0.46822 | 0.00492 | 6.3109e-35 |
| RealHAAR | 0.99596 | 0.94456 | 0.01081 | 0.35675 |
| RandDCT | 0.99773 | 0.93859 | 0.01156 | 0.18737 |

Table 2: Results of Test 1 for $\gamma = 0.5$ and $\beta = 0.8$.

Reproducibility advisory. All the figures and tables in this paper, including those in the Supporting Information, are fully reproducible from our raw results

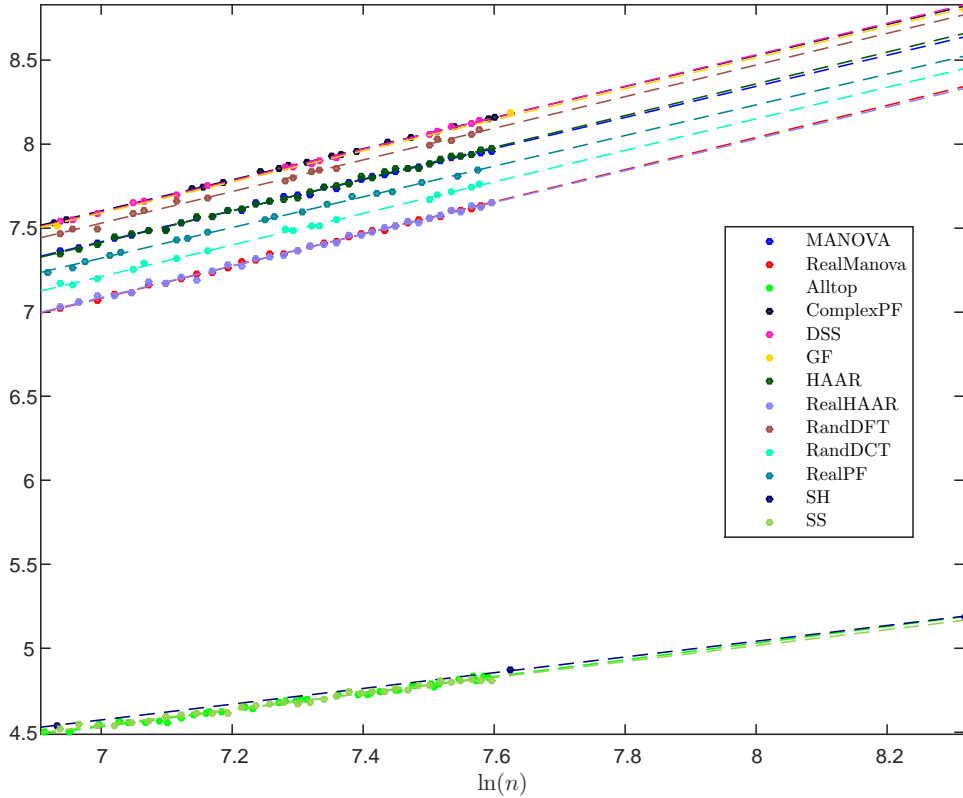


Figure 4: Test 1 for $\gamma = 0.5$ and $\beta = 0.8$. Plot shows $-\frac{1}{2} \ln \text{Var}_K(\Delta_{KS}(X_K^{(n)}))$ over $\ln(n)$.

and code deposited in the Data and Code Supplement [39].

Discussion

The hypotheses

Our Universality Hypotheses may be surprising in several aspects: Firstly, the frames examined were designed to minimize frame bounds and worse-case pairwise correlations. Still it appears that they perform well when the performance criterion is based on spectrum of the typical selection of k frame vectors. Secondly, under the Universality Hypotheses, all these deterministic frames perform exactly as well as random frame designs such as the random Fourier frame. Inasmuch as frames are continuous codes, we find deterministic codes matching the performance of random codes. Finally, the Hypotheses suggest an extremely broad universality property: many different ensembles of random matrices asymptotic exhibit the limiting MANOVA spectrum.

All of the deterministic frames under study satisfy the Universality Hypotheses (with Hypothesis **H4** satisfied only for ETFs). This should not give the impression that *any* deterministic frame satisfies these hypotheses! Firstly, because the empirical measures of an arbitrary sequence of frames rarely converge (thus

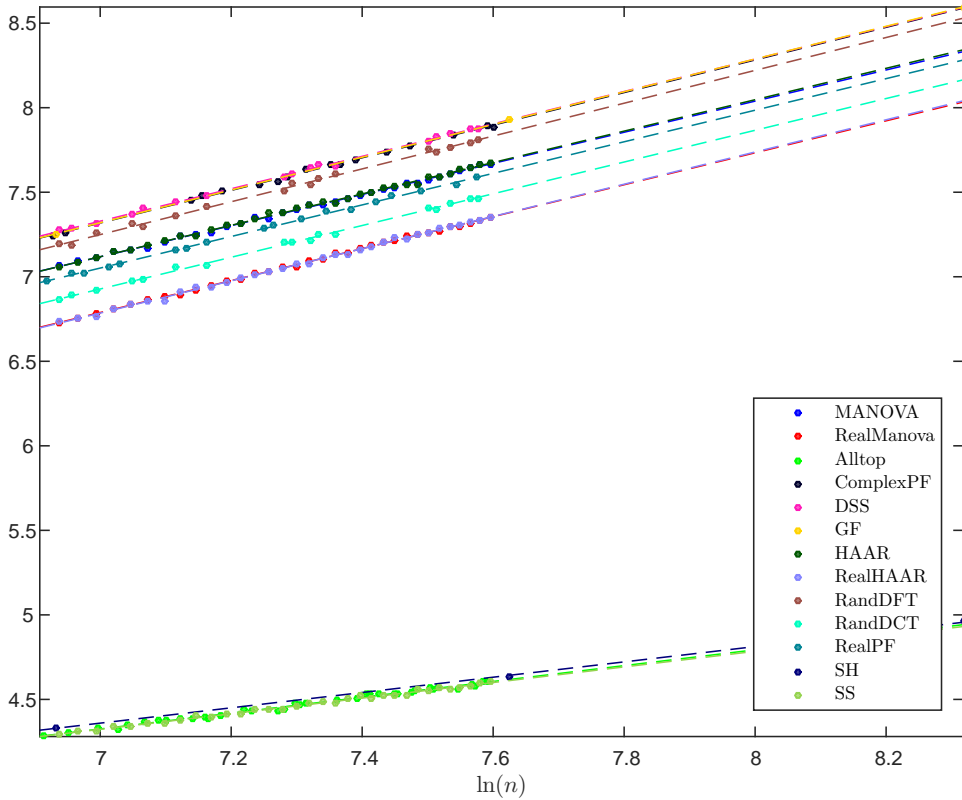


Figure 5: Test 1 for $\gamma = 0.5$ and $\beta = 0.6$. Plot shows $-\frac{1}{2} \ln \text{Var}_K(\Delta_{KS}(X_K^{(n)}))$ over $\ln(n)$.

violating Hypothesis H1). Secondly, even if they converge, a too-simplistic frame design often leads to concentration of the lower edge of the empirical spectrum near zero, resulting in a non-MANOVA spectrum and poor performance. For example, if the frame is sparse, say, consisting of some m columns of the n -by- n identity matrix, then a fraction $(n - m)/n$ of the singular values of a typical submatrix are exactly zero.

The frames under study are all ETFs or near-ETFs, all with favorable frame properties. To make this point, we have included in the Supporting Information [40] study of a low-pass frame, in which the Fourier frequencies included in the frame are the lowest ones. This is in contrast with the clever choice of frequencies leading to the difference-set spectrum frame (DSS). Indeed the low-pass frame does not have appealing frame properties. It's quite obvious from the results in the SI, as well as results regarding the closely related random Vandermonde ensemble [36], that such frames do not satisfy any of the Universality Hypotheses **H2–H6**.

We note that convergence rates of the form (12) and (13) are known for other classical random matrix ensembles [32–35].

We further note that Hypotheses **H1–H4** do not imply Hypotheses **H5–H6**. Even if the empirical CDF converges in KS metric to the limiting $\text{MANOVA}(\beta, \gamma)$ distribution, functionals which are not continuous in the KS metric do not neces-

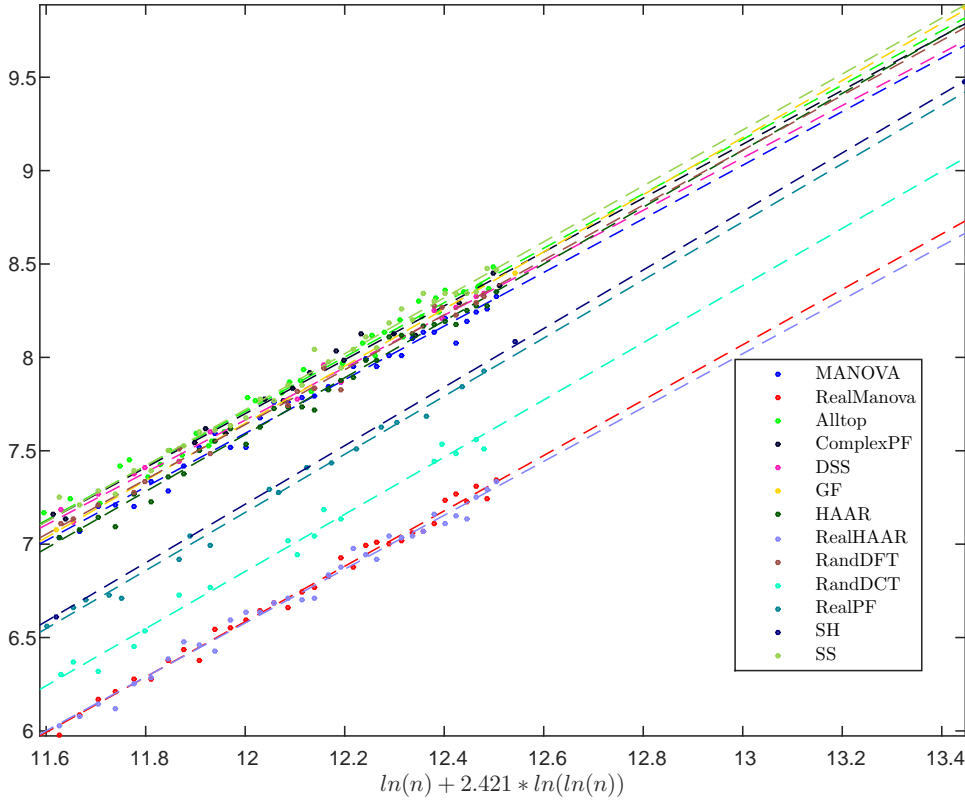


Figure 6: Test 2 for Ψ_{AC} , $\gamma = 0.5$ and $\beta = 0.8$. Plot shows $-\ln \mathbb{E}_K(\Delta_\Psi(X_K^{(n)})^2)$

sarily converge, and moreover no uniform rate of convergence is a-priori implied.

Our contributions

This paper presents a novel, simple method for approximate computation (with known and good approximation error) of spectral functionals of k -submatrix ensemble for a variety of random and deterministic frames, using (1). Our results make it possible to tabulate these approximate values, creating a useful resource for scientists. As an example, we include Table 5. This is a lookup table for the value of the functional Ψ_{AC} on the difference-set spectrum deterministic frame family (DSS), listing by values of n and k the asymptotic (approximate) value calculated analytically from the limiting $f_{\beta,\gamma}^{MANOVA}$ distribution, and the standard approximation error.

To this end we developed a systematic empirical framework, which allows validation of (1) and discovery of the exponents there. Our work is fully reproducible, and our framework is available (along with the rest of our results and code) in the Code and Data Supplement [39]. In addition, our results provide overwhelming empirical evidence for a number of phenomena, which were, to the best of knowledge, previously unknown:

1. **The typical k -submatrix ensemble of deterministic frames is an object of interest.** While there is absolutely no randomness involved in the submatrix

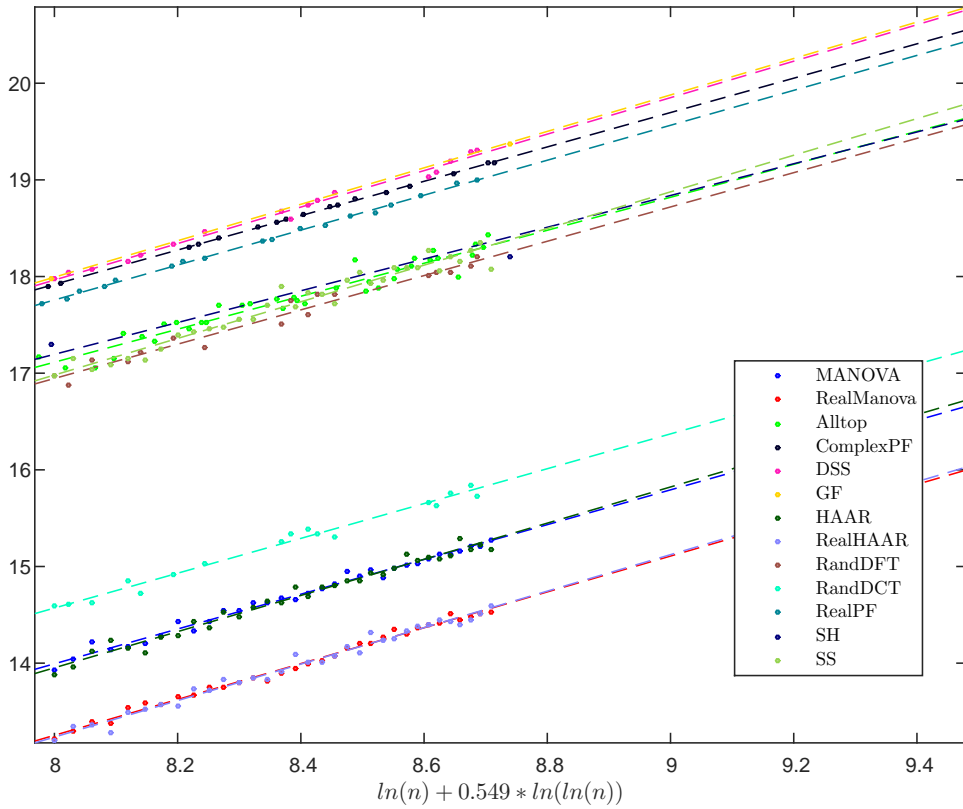


Figure 7: Test 2 for $\Psi_{Shannon}$, $\gamma = 0.5$ and $\beta = 0.8$. Plot shows $-\ln \mathbb{E}_K(\Delta_\Psi(X_K^{(n)})^2)$

X_K of a deterministic frame (other than the choice of subset K), the typical k -submatrix appears to be an ensemble in its own right, with properties so far attributed only to random matrix ensembles – including a universal, compactly-supported limiting spectral distribution and convergence of the maximal (resp. minimal) singular value to the upper (resp. lower) edges of the limiting distribution.

2. **MANOVA(β, γ) as a universal limiting spectral distribution.** Wachter's MANOVA(β, γ) distribution is the limiting spectral distribution of $\lambda(G_K)$, as $k/m \rightarrow \beta$ and $m/n \rightarrow \gamma$, for the typical k -submatrix ensemble of deterministic frames (including difference-set, Grassmannian, real Paley, complex Paley, quadratic chirp, spiked and sines, and spikes and Hadamard). The same is true for real random frames - random cosine transform and random Haar.
3. **Convergence of the edge-spectrum.** For all the deterministic frames above, as well as for the random frames (random cosine, random Fourier, complex Haar, real Haar), the maximal and minimal eigenvalues of the k -typical submatrix ensemble converge to the support-edges of the MANOVA(β, γ) limiting distribution. The convergence follows a universal power-law rate.
4. **A definite power-law rate of convergence for the entire spectrum of the**

| Frame | R^2 | \hat{b} | $SE(\hat{b})$ | p-value $b = b_{MANOVA}$ |
|------------|---------|-----------|---------------|-----------------------------|
| MANOVA | 0.98721 | 1.79936 | 0.03678 | 1 |
| DSS | 0.99110 | 1.88674 | 0.04615 | 0.14551 |
| GF | 0.99997 | 1.88548 | 0.01073 | 0.03161 |
| ComplexPF | 0.99977 | 1.77783 | 0.00701 | 0.56808 |
| Alltop | 0.93841 | 1.70618 | 0.07388 | 0.26297 |
| SS | 0.95539 | 1.89501 | 0.07355 | 0.24922 |
| HAAR | 0.97971 | 1.87082 | 0.04836 | 0.24400 |
| RandDFT | 0.96928 | 1.77454 | 0.08157 | 0.78270 |
| RealMANOVA | 0.99202 | 2.05451 | 0.03309 | 1 |
| RealPF | 0.99834 | 2.00345 | 0.02045 | 0.19576 |
| SH | 0.97850 | 1.81297 | 0.26874 | 0.37904 |
| RealHAAR | 0.98287 | 2.09078 | 0.04958 | 0.54503 |
| RandDCT | 0.98364 | 1.99663 | 0.06648 | 0.43977 |

Table 3: Results of Test 2 for $\Psi_{Shannon}$, $\gamma = 0.5$ and $\beta = 0.8$

MANOVA(n, m, k, \mathcal{F}) ensemble to its MANOVA(β, γ) limit, with different exponents in the real and the complex cases.

- 5. Universality of the power-law exponents for the entire spectrum.** The complex deterministic ETF frames (difference-set, Grassmannian, complex Paley) share the power-law exponents with the MANOVA(n, m, k, \mathbb{C}) ensemble. The same is true for the complex random frames (random Fourier and complex Haar). The complex tight non-equiangular Alltop frame, which can be constructed for various aspect ratios, also share the power-law exponents with the MANOVA(n, m, k, \mathbb{C}) ensemble for $\gamma < 0.5$. The real deterministic ETF frame (real Paley) shares the exponent with the MANOVA(n, m, k, \mathbb{R}). The same is true for real random frames (random cosine and real Haar). All non-ETFs under study, with $\gamma = 0.5$, share different power-law exponents (slower convergence).
- 6. A definite power-law rate of convergence for functionals** including Ψ_{StRIP} , Ψ_{AC} and $\Psi_{Shannon}$.
- 7. Universality of the power-law exponents for functionals.** For practically all frames under study, both random and deterministic, the power-law exponents for functionals agree with those of the MANOVA(n, m, k, \mathbb{R}) (real frames) and MANOVA(n, m, k, \mathbb{C}) (complex frames).

Intercepts

Our results showed a surprising categorization of the deterministic and random frames under study, according to the constant C in (12), or equivalently, according to the intercept (vertical shift) in the linear regression on $\log(n)$. Figure 4

and Figure 5 clearly show that the regression lines, while having identical slopes (as predicated by Hypothesis **H3**), are grouped according to their intercepts into the following seven categories: Complex MANOVA ensemble and complex Haar (Manova, HAAR); Real MANOVA ensemble and real Haar (RealManova, Real-HAAR); Complex ETFs (DSS, GF, ComplexPF); Non-ETFs (SS,SH,Alltop); Real ETF (RealPF); Complex Random Fourier (RandDFT), and Real Random Fourier (RandDCT).

Interestingly, intercepts of all complex frames are larger (meaning that the linear coefficient C in (12) is smaller) than those of all real frames. Also, the less randomness exists in the frame, the higher the intercept: intercepts of deterministic ETFs are higher than those of random Fourier and random Cosine, which are in turn higher than those of Haar frames and the MANOVA ensembles.

Related work

Farrell [6] has conjectured that the phenomenon of convergence of the spectrum of typical k -submatrices to the limiting MANOVA distribution is indeed much broader and extends beyond the partial Fourier frame he considered. A related empirical study was conducted by Monajemi et al [5]. There, the authors considered the so-called sparsity-undersampling phase transition in compressed sensing. This asymptotic quantity poses a performance criterion for frames that interacts with the typical k -submatrix X_K in a manner possibly more complicated than the spectrum $\lambda(G_K)$. The authors investigated various deterministic frames, most of which are studied in this paper, and brought empirical evidence that the phase transition for each of these deterministic frames is identical to the phase transition of Gaussian frames. Gurevich and Hadani [12] proposed certain deterministic frame construction and effectively proved that the empirical spectral distribution of their typical k -submatrix converges to a semicircle, assuming $k = m^{1-\varepsilon}$, a scaling relation different than the one considered here. [37] and [38] also considered deterministic frame designs, chirp sensing codes and binary linear codes, with a random sampling. In their design the aspect ratios are large (e.g., in [37] $m \sim k^2$ and $n \sim m^2$), so the spectrum converges to the Marčenko-Pastur distribution. Tropp [30] provided bounds for $\lambda_{max}(G_K)$ and $\lambda_{min}(G_K)$ when X is a general dictionary. Collins [25] has shown that the spectrum of a matrix model deriving from random projections has the same eigenvalue distribution of the MANOVA ensemble in finite n . Wachter [27] used a connection between the MANOVA ensemble and submatrices of Haar matrices to derive the asymptotic spectral distribution $\text{MANOVA}(\beta, \gamma)$.

Conclusions

We have observed a surprising universality property for the k -submatrix ensemble corresponding to various well-known deterministic frames, as well as to well-known random frames. The MANOVA ensemble, and the MANOVA limiting

distribution, emerge as key objects in the study of frames, both random and deterministic, in the context of sparse signals and erasure channels. We hope that our findings will invite rigorous mathematical study of these fascinating phenomena.

In any frame where our Universality Hypotheses hold (including all the frames under study here), Figure 2 correctly describes the limiting values of f_{RIP} , f_{AC} and $f_{Shannon}$ and shows that codes based on deterministic frames (involving no randomness and allowing fast implementations) are better, across performance measures, than i.i.d random codes.

The empirical framework we proposed in this paper may be easily applied to new frame families $X^{(n)}$ and new functionals Ψ , extending our results further and mapping the frontiers of the new universality property. In any frame family, and for any functional, where our Universality Hypotheses hold, we have proposed a simple, effective method for calculating quantities of the form $\mathbb{E}_K \Psi(\lambda(G_K))$ to known approximation, which improves polynomially with n .

Acknowledgements

The authors thank David Donoho for numerous helpful suggestions and the anonymous referees for their helpful comments. This work was partially supported by Israeli Science Foundation grant no. 1523/16.

| Frame | $b_{spectrum}$ | $b_{\Psi_{RIP}}$ | $a_{\Psi_{RIP}}$ | $b_{\Psi_{AC}}$ | $a_{\Psi_{AC}}$ | b_{Ψ_S} | a_{Ψ_S} | $b_{\Psi_{max}}$ | $a_{\Psi_{max}}$ | $b_{\Psi_{min}}$ | $a_{\Psi_{min}}$ | $b_{\Psi_{cond}}$ | $a_{\Psi_{cond}}$ |
|------------|----------------|------------------|------------------|-----------------|-----------------|--------------|--------------|------------------|------------------|------------------|------------------|-------------------|-------------------|
| MANOVA | 0.93 | 1.15 | 2.21 | 1.44 | 3.48 | 1.80 | 0.99 | 1.13 | 2.48 | 1.00 | 3.09 | 1.87 | -4.55 |
| DSS | 0.94 | 1.14 | 2.18 | 1.40 | 3.40 | 1.89 | 1.04 | 1.10 | 2.41 | 1.00 | 3.11 | 1.87 | -4.56 |
| GF | 0.92 | 1.17 | 2.23 | 1.53 | 3.70 | 1.89 | 1.03 | 1.13 | 2.48 | 1.04 | 3.22 | 1.95 | -4.76 |
| ComplexPF | 0.92 | 1.13 | 2.17 | 1.44 | 3.49 | 1.78 | 0.98 | 1.10 | 2.41 | 1.00 | 3.12 | 1.87 | -4.56 |
| Alltop | 0.50 | 1.14 | 2.18 | 1.46 | 3.53 | 1.71 | 0.94 | 1.11 | 2.42 | 1.01 | 3.13 | 1.86 | -4.54 |
| SS | 0.47 | 1.11 | 2.13 | 1.50 | 3.63 | 1.90 | 1.04 | 1.08 | 2.36 | 0.98 | 3.06 | 1.83 | -4.47 |
| HAAR | 0.94 | 1.10 | 2.11 | 1.52 | 3.69 | 1.87 | 1.03 | 1.09 | 2.37 | 1.01 | 3.13 | 1.88 | -4.59 |
| RandDFT | 0.94 | 1.21 | 2.32 | 1.47 | 3.56 | 1.77 | 0.97 | 1.11 | 2.42 | 1.03 | 3.18 | 1.93 | -4.70 |
| RealMANOVA | 0.96 | 0.87 | 3.58 | 1.26 | 5.21 | 1.27 | 5.26 | 0.90 | 3.73 | 0.87 | 3.58 | 0.77 | 3.17 |
| RealPF | 0.91 | 0.92 | 3.82 | 1.32 | 5.46 | 1.24 | 5.12 | 0.94 | 3.88 | 0.94 | 3.88 | 0.81 | 3.36 |
| SH | 0.47 | 0.93 | 3.82 | 1.34 | 5.53 | 1.14 | 4.71 | 0.93 | 3.82 | 0.93 | 3.82 | 0.85 | 3.51 |
| RealHAAR | 0.94 | 0.86 | 3.54 | 1.23 | 5.07 | 1.29 | 5.35 | 0.89 | 3.68 | 0.90 | 3.73 | 0.79 | 3.28 |
| RandDCT | 0.94 | 0.99 | 4.08 | 1.30 | 5.38 | 1.24 | 5.10 | 0.94 | 3.89 | 0.95 | 3.93 | 0.82 | 3.40 |

Table 4: Summary of universal exponents for convergence. $\gamma = 0.5, \beta = 0.8, (\Psi_S = \Psi_{Shannon})$.

| n | 1031 | 1151 | 1291 | 1451 | 1571 | 1811 | 1951 |
|---------------------|-------------------|-------------------|-------------------|-------------------|-------------------|-------------------|-------------------|
| RMSE, $\beta = 0.8$ | 3 ± 0.0281 | 3 ± 0.0253 | 3 ± 0.0227 | 3 ± 0.0204 | 3 ± 0.0189 | 3 ± 0.0166 | 3 ± 0.0155 |
| RMSE, $\beta = 0.6$ | 1.75 ± 0.0073 | 1.75 ± 0.0065 | 1.75 ± 0.0058 | 1.75 ± 0.0051 | 1.75 ± 0.0048 | 1.75 ± 0.0041 | 1.75 ± 0.0038 |

Table 5: $\Psi(f_{\beta,\gamma}^{MANOVA}) \pm \sqrt{\Delta_{\Psi}(X_{K_n}^{(n)}; n, m_n, k_n)^2}$ for Ψ_{AC} and DSS frame, $m = \frac{n-1}{2}$, $k = \beta \cdot m$.

References

- [1] Forrester, P. J. (2010). *Log-gases and random matrices (LMS-34)*. Princeton University Press.
- [2] Candes, E. J. (2008). The restricted isometry property and its implications for compressed sensing. *Comptes Rendus Mathematique*, 346(9), 589-592.
- [3] Haikin, M., Zamir, R. (2016). Analog Coding of a Source with Erasures. In *IEEE International Symposium on Information Theory Proceedings (ISIT)* (pp. 2074-2078). IEEE.
- [4] Tulino, A. M., Verdú, S. (2004). *Random matrix theory and wireless communications* (Vol. 1). Now Publishers Inc.
- [5] Monajemi, H., Jafarpour, S., Gavish, M., Donoho, D. L. (2013). Deterministic matrices matching the compressed sensing phase transitions of Gaussian random matrices. *Proceedings of the National Academy of Sciences*, 110(4), 1181-1186.
- [6] Farrell, B. (2011). Limiting empirical singular value distribution of restrictions of discrete Fourier transform matrices. *Journal of Fourier Analysis and Applications*, 17(4), 733-753.
- [7] Xia, P., Zhou, S., Giannakis, G. B. (2005). Achieving the Welch bound with difference sets. *IEEE Transactions on Information Theory*, 51(5), 1900-1907.
- [8] Strohmer, T., Heath, R. W. (2003). Grassmannian frames with applications to coding and communication. *Applied and computational harmonic analysis*, 14(3), 257-275.
- [9] Paley, R. E. (1933). On orthogonal matrices. *Journal of Mathematics and Physics*, 12(1), 311-320.
- [10] Calderbank, R., Howard, S., Jafarpour, S. (2010). Construction of a large class of deterministic sensing matrices that satisfy a statistical isometry property. *IEEE journal of selected topics in signal processing*, 4(2), 358-374.
- [11] Johnstone, I. M. (2008). Multivariate analysis and Jacobi ensembles: Largest eigenvalue, Tracy–Widom limits and rates of convergence. *Annals of statistics*, 36(6), 2638.
- [12] Gurevich, S., Hadani, R. (2008). The statistical restricted isometry property and the Wigner semicircle distribution of incoherent dictionaries. *arXiv preprint arXiv:0812.2602*.
- [13] Marčenko, V. A., Pastur, L. A. (1967). Distribution of eigenvalues for some sets of random matrices. *Mathematics of the USSR-Sbornik*, 1(4), 457.

- [14] Haviv, I., Regev, O. (2016, January). The restricted isometry property of subsampled Fourier matrices. In *Proceedings of the Twenty-Seventh Annual ACM-SIAM Symposium on Discrete Algorithms* (pp. 288-297). SIAM.
- [15] Donoho, D. L., Elad, M., Temlyakov, V. N. (2006). Stable recovery of sparse overcomplete representations in the presence of noise. *IEEE Transactions on information theory*, 52(1), 6-18.
- [16] Mazumdar, A., Barg, A. (2011, July). General constructions of deterministic (s) rip matrices for compressive sampling. In *IEEE International Symposium on Information Theory Proceedings (ISIT)* (pp. 678-682). IEEE.
- [17] Bandeira, A. S., Fickus, M., Mixon, D. G., Wong, P. (2013). The road to deterministic matrices with the restricted isometry property. *Journal of Fourier Analysis and Applications*, 19(6), 1123-1149.
- [18] Fickus, M., Jasper, J., Mixon, D. G., Peterson, J. (2015). Group-theoretic constructions of erasure-robust frames. *Linear Algebra and its Applications*, 479, 131-154.
- [19] Rudelson, M., Vershynin, R. (2008). On sparse reconstruction from Fourier and Gaussian measurements. *Communications on Pure and Applied Mathematics*, 61(8), 1025-1045.
- [20] Candes, E. J., Tao, T. (2006). Near-optimal signal recovery from random projections: Universal encoding strategies?. *IEEE transactions on information theory*, 52(12), 5406-5425.
- [21] Nelson, J., Price, E., Wootters, M. (2014, January). New constructions of RIP matrices with fast multiplication and fewer rows. In *Proceedings of the Twenty-Fifth Annual ACM-SIAM Symposium on Discrete Algorithms* (pp. 1515-1528). SIAM.
- [22] Pfander, G. E., Rauhut, H., Tropp, J. A. (2013). The restricted isometry property for time-frequency structured random matrices. *Probability Theory and Related Fields*, 156(3-4), 707-737.
- [23] Edelman, A., Sutton, B. D. (2008). The beta-Jacobi matrix model, the CS decomposition, and generalized singular value problems. *Foundations of Computational Mathematics*, 8(2), 259-285.
- [24] Cheraghchi, M., Guruswami, V., Velingker, A. (2013). Restricted isometry of Fourier matrices and list decodability of random linear codes. *SIAM Journal on Computing*, 42(5), 1888-1914.
- [25] Collins, B. (2005). Product of random projections, Jacobi ensembles and universality problems arising from free probability. *Probability theory and related fields*, 133(3), 315-344.

- [26] Foucart, S., Lai, M. J. (2009). Sparsest solutions of underdetermined linear systems via ℓ_q -minimization for $0 < q \leq 1$. *Applied and Computational Harmonic Analysis*, 26(3), 395-407.
- [27] Wachter, K. W. (1980). The limiting empirical measure of multiple discriminant ratios. *The Annals of Statistics*, 937-957.
- [28] Bai, Z., Silverstein, J. W. (2010). *Spectral analysis of large dimensional random matrices* (Vol. 20). New York: Springer.
- [29] Yao, J., Bai, Z., Zheng, S. (2015). *Large Sample Covariance Matrices and High-Dimensional Data Analysis* (No. 39). Cambridge University Press.
- [30] Tropp, J. A. (2008). On the conditioning of random subdictionaries. *Applied and Computational Harmonic Analysis*, 25(1), 1-24.
- [31] Elad, M. (2010). *Sparse and Redundant Representations: From Theory to Applications in Signal and Image Processing*. Springer New York.
- [32] Götze, F., Tikhomirov, A. (2011). On the Rate of Convergence to the Marchenko–Pastur Distribution. *arXiv preprint arXiv:1110.1284*.
- [33] Götze, F., Tikhomirov, A. (2016). Optimal bounds for convergence of expected spectral distributions to the semi-circular law. *Probability Theory and Related Fields*, 165(1-2), 163-233.
- [34] Chatterjee, S., Bose, A. (2004). A new method for bounding rates of convergence of empirical spectral distributions. *Journal of Theoretical Probability*, 17(4), 1003-1019.
- [35] Meckes, E. S., Meckes, M. W. (2016). Rates of convergence for empirical spectral measures: a soft approach. *arXiv preprint arXiv:1601.03720*.
- [36] Debbah, M. (2008). Asymptotic Behaviour of Random Vandermonde Matrices with Entries on the Unit Circle. *arXiv preprint arXiv:0802.3570*.
- [37] Applebaum, L., Howard, S. D., Searle, S., Calderbank, R. (2009). Chirp sensing codes: Deterministic compressed sensing measurements for fast recovery. *Appl. Comp. Harmonic Analysis*, 26(2), 283-290.
- [38] Babadi, B., Tarokh, V. (2011). Spectral distribution of random matrices from binary linear block codes. *IEEE Trans. Info. Theory*, 57(6), 3955-3962.
- [39] Code and Data Supplement for “Random Subsets of Deterministic Frames have MANOVA Spectra”. Available online at <https://purl.stanford.edu/qg138qm8653>
- [40] Supplementary Information for “Random Subsets of Deterministic Frames have MANOVA Spectra”. Available online at <https://purl.stanford.edu/qg138qm8653>